Journal of Molecular Catalysis B: Enzymatic 71 (2011) 159–165

Contents lists available at ScienceDirect

Journal of Molecular Catalysis B: Enzymatic

journal homepage: www.elsevier.com/locate/molcatb

NAD(P)H oxidase V from *Lactobacillus plantarum* (NoxV) displays enhanced operational stability even in absence of reducing agents

Jonathan T. Park[a], Jun-Ichiro Hirano[a,1], Vaijayanthi Thangavel[a,2], Bettina R. Riebel[b], Andreas S. Bommarius[a,c,*]

[a] School of Chemical & Biomolecular Engineering, Parker H. Petit Institute of Bioengineering and Biosciences, Georgia Institute of Technology, 315 Ferst Drive, Atlanta, GA 30332-0363, USA
[b] Department of Pathology, Whitehead Building, Emory University, 615 Michael Drive, Atlanta, GA, 30322, USA
[c] School of Chemistry and Biochemistry, Georgia Institute of Technology, 901 Atlantic Drive, Atlanta, GA 30332-0400, USA

ARTICLE INFO

Article history:
Received 4 January 2011
Received in revised form 9 April 2011
Accepted 11 April 2011
Available online 17 April 2011

Keywords:
NADH oxidase
Cofactor
Cofactor regeneration
Cofactor specificity
Overoxidation
Total turnover number

ABSTRACT

Active pharmaceutical ingredients (APIs) such as L-sugars and keto acids are favorably accessed through selective oxidation of sugar alcohols and amino acids, respectively, catalyzed by NAD(P)-dependent dehydrogenases. Cofactor regeneration from NAD(P)H conveniently is achieved via water-forming NAD(P)H oxidases (nox2), which only need molecular oxygen as co-substrate. Turnover-dependent overoxidation of the conserved cysteine residue in the active site of water-forming NADH oxidases is the presumed cause of the limited nox2 stability.

We present a novel NAD(P)H oxidase, NoxV from *Lactobacillus plantarum*, with specific activity of 167 U/mg and apparent kinetic constants at air saturation and 25 °C of $k_{cat,app} = 212\ s^{-1}$ and $K_{M,app} = 50.2\ \mu M$ in the broad pH optimum from 5.5 to 8.0. The enzyme features a higher stability than other NAD(P)H oxidases against overoxidation, as is evidenced by a higher total turnover number, in the presence (168,000) and, most importantly, also in the absence (128,000) of exogenously added reducing agents. While the native enzyme shows exclusively activity on NADH, we engineered the substrate binding pocket to generate variants, G178K,R and L179K,R,H that accommodate and oxidize both NADH and NADPH as substrates.

1. Introduction

Enzymatic synthesis steps are used to produce active pharmaceutical ingredients (APIs) at higher yields, greater selectivity, and greater productivity than is possible through isolation of natural sources or chemically catalyzed routes. Interest in the nicotinamide cofactor aided production of rare sugars, namely L-nucleosides, for example L-ribose, L-mannose and L-gulose, has arisen for a number of L-nucleoside-based pharmaceutical compounds, such as the hepatitis B drug Emtriva® and the human immunodeficiency virus drug Clevudine®. A number of such rare sugar-based pharmaceuticals are currently approved or in clinical trials [1]. Another example of cofactor-assisted API synthesis is the production of keto acids, which are used to treat mild chronic renal insufficiency of hemodialysis patients and hyperphosphatemia [2,3]. Thus, α-ketoglutarate can be synthesized enzymatically from mono sodium L-glutamate (MSG) using L-glutamate dehydrogenase and a nicotinamide cofactor [4].

High costs of nicotinamide cofactors (NAD^+: $30/g; $NADP^+$: $230/g from laboratory suppliers) rule out the option of adding equimolar amounts for large-scale processes. A regeneration system is mandatory for advantageous economics but also often alleviates product inhibition, and acts as the driving force to overcome thermodynamic equilibrium limitations [6]. Enzymatic, chemical, electrochemical, photochemical, and biological methods have been proposed for cofactor regeneration [5–7].

Among different systems that can be chosen for cofactor regeneration, NAD(P)H oxidases feature a number of benefits, as they utilize only NAD(P)H and oxygen as co-substrates, both of which are available intracellularly (Fig. 1), thus obviating exogenous addi-

Abbreviations: API, active pharmaceutical ingredient; BME, β-mercaptoethanol; DTT, dithiothreitol; NoxV, NADH oxidase from *L. plantarum* V; SDS-PAGE, sodium dodecyl sulfate polyacrylamide gel electrophoresis; TTN, total turnover number; T_{50}^{30}, temperature exhibiting half of the original activity after 30 min; Enzymes, E.C. 1.6.–.–NADH oxidase.

* Corresponding author at: School of Chemical and Biomolecular Engineering and School of Chemistry and Biochemistry, Parker H. Petit Institute for Bioengineering and Bioscience, Georgia Institute of Technology, 315 Ferst Drive, Atlanta, GA 30332-0363, USA. Fax: +1 404 894 2291.
E-mail address: andreas.bommarius@chbe.gatech.edu (A.S. Bommarius).
[1] Current address: Mitsubishi Chemical Corporation, 14-1 Shiba 4-chome, Minato-ku, Tokyo, 108-0014, Japan.
[2] Current address: Department of Chemistry, Graduate School of Science, Kyoto University, Kitashirakawa-Oiwakecho, Sakyo-Ku, Kyoto 606-8502, Japan

1381-1177/$ – see front matter © 2011 Elsevier B.V. All rights reserved.
doi:10.1016/j.molcatb.2011.04.013

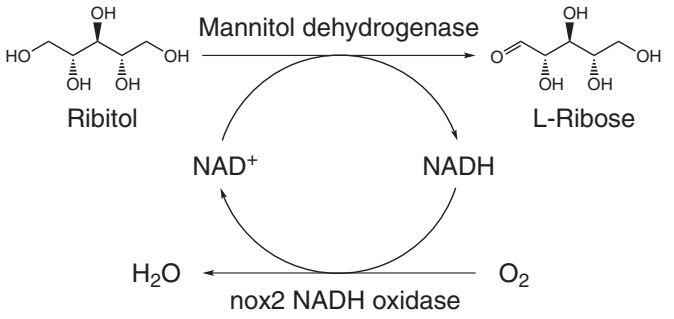

Fig. 1. Schematic conversion of ribitol to L-ribose through mannitol-1-dehydrogenase from *Apium graveolens* complemented with NADH cofactor regeneration using nox2 NADH oxidase.

tion, and, in the case of nox2 NAD(P)H oxidases, produce only water next to $NAD(P)^+$ [8]. The reaction is carried out in a purely aqueous phase (in the absence of harsh solvents and metal catalysts).

All previously discovered nox2 NAD(P)H oxidases utilize FAD as a cofactor, and have a conserved cysteine residue that is catalytically active [9–12]. During catalysis, the thiol (–SH) or thiolate ($–S^-$) is oxidized to sulfenic acid (–SOH) and reduced back to the thiol/ate as a part of the NAD(P)H reduction mechanism. During this redox cycle the cysteine can also be overoxidized, producing a sulfinic ($–SO_2H$) and then a sulfonic acid ($–SO_3H$), and thereby deactivating the enzyme [13]. Overoxidation of this cysteine residue can be decelerated by employing exogenous reducing agents such as dithiothreitol (DTT) or β-mercaptoethanol (BME) [4]. This overoxidation of the catalytically active cysteine is the presumed cause of turnover-limited operational stability of nox2 proteins [4,14]. Thus, reducing agents have shown to extend the useful active enzyme lifetime and its total turnover number (TTN), a measure of operational stability.

The *NoxV* gene codes for an annotated NADH oxidase (NoxV) from *Lactobacillus plantarum* consisting of 1350 bp with a predicted size of 49 kDa. This study investigates the enzymatic properties of NoxV. A higher enzymatic productivity is achieved compared to its analogs, as evidenced by NoxV's higher TTN and increased stability against over-oxidation. Furthermore, while the wildtype enzyme solely accepts NADH as a substrate, we engineered the substrate binding pocket so that the enzyme also accepts and oxidizes NADPH.

2. Experimental

2.1. Enzymes and other materials

The gene of NADH oxidase V (*NoxV*) from *L. plantarum* 10S was obtained via gene probe from genomic DNA from the American Type Culture Collection (Manassas, VA), ATCC 10012. NADH and NADPH were obtained from Amresco (Solon, OH) and EMD chemicals (Gibbstown, NJ), respectively. MagicMedia™ *Escherichia coli* Expression Medium was purchased from Invitrogen (Carlsbad, CA). Molecular biology reagents such as DTT were obtained from JT Baker (Phillipsburg, NJ), all other materials such as various salts used for buffers, BME and NAD^+ were obtained from Sigma–Aldrich (St. Louis, MO). Oligonucleotides for cloning were purchased from Eurofins-mwg|operon Biosciences (Huntsville, AL).

2.2. Cloning

The gene was cloned through PCR using the following primers; forward (5′-TGCATGCATGCCATGGTTATGAAAGTTATTGTAATTGGTTGTACCCA-3′) and reverse (5′-CCGCCGCCGCCGCTCGAGTTATTCAGTGACAGCTTCGGCC-3′) with NcoI and XhoI, underlined, as restriction sites used for restriction and ligation. The PCR product was gel purified with a Qiagen gel extraction kit and cloned into a pET-28a vector (Novagen; Darmstadt, Germany). The plasmid was then transformed into *E. coli* BL21(DE3)pLysS for expression. Constructs were confirmed with sequencing through Eurofins-mwg|operon Biosciences (Huntsville, AL).

2.3. Site-directed mutagenesis

Single and double mutations were performed on residues G178 and L179 into K, R and K, R, H, respectively, through overlap and Quikchange® PCR protocol using the following forward primers and their complementary reverse primers; G178ARR (5′-GCAAGGTAAGGAAGTCACACTAATTGATARRTTACCACGGATTTTAAATAAATACTTAGACAA-3′), L179CRY (5′-AGGTAAGGAAGTCACACTAATTGATGGTCRYCCACGGATTTTAAATAAATACTTAGACAAAG-3′), L179K (5′-AGGTAAGGAAGTCACACTAATTGATGGTAAACCACGGATTTTAAATAAATACTTAGACAAA-3′), G178ARR/L179CRY (5′-GCAAGGTAAGGAAGTCACACTAATTGATARRCRYCCACGGATTTTAAATAAATACTTAGACAAAG-3′), G178ARR/L179K (5′-GCAAGGTAAGGAAGTCACACTAATTGATARRAAACCACGGATTTTAAATAAATACTTAGACAAA-3′). Degenerate codons were used to generate multiple mutants with single transformations. ARR codes for amino acids R and K, and CRY codes H and R. The DNA from PCR was transformed into *E. coli* XL1-blue. Colonies were picked from agar plates and sent for sequencing to Eurofins-mwg|operon Biosciences (Huntsville, AL).

2.4. Overexpression

Growth and overexpression was carried out in MagicMedia™ *E. coli* Expression Medium (Invitrogen; Carlsbad, CA) with a final concentration of 30 μg mL^{-1} each of kanamycin and chloramphenicol. A dual temperature protocol was used for growth, starting out at 30 °C for 6 h, and then continued at room temperature (25 ± 2 °C) for an additional 22 h. Cultures were harvested by centrifugation in a Beckman centrifuge at 4050 *g* for 20 min in 50 mL conical tubes. The resulting cell pellet was either frozen, and stored at −80 °C or purified directly as described below.

2.5. Purification

Purification of NoxV was carried out at 4 °C or on ice to prevent denaturation of the enzyme. Cell pellets were resuspended in 15 mL of 10 mM Tris–Cl buffer, pH 7.5 with 5 mM DTT (Buffer A) and sonicated at 14 W for 30 s nine times. Sonicated cells were centrifuged at 18,500 *g* for 30 min. The clarified cell lysate was then dialyzed against 250 mL of buffer A with 50% ammonium sulfate for 2 h. The dialysis membrane was transferred to fresh buffer and further dialyzed for 2 h. The solution was then centrifuged at 18,500 *g* for 30 min. The resulting supernatant was filtered through a 0.8 μm and 0.2 μm microfiltration membranes in series. The filtrate was loaded onto a HiPrep 16/10 butyl hydrophobic interaction column on an ÄKTAexplorer™. A gradient separation was performed starting from buffer A with 30% ammonium sulfate to 15%. The fractions with the highest activity were collected and dialyzed against buffer A for 2 h. After exchanging to fresh buffer the sample was dialyzed for an additional 2 h. The sample was loaded on a HiPrep 16/10 DEAE weak anionic exchange column on the ÄKTAexplorer™. Separation was achieved with buffer A containing NaCl, a gradient of 150–250 mM. The resulting fractions were assayed and the ones with highest activity were collected as pure protein. The purified protein was either stored in 4 °C or in −20 °C with 25% glycerol.

2.6. Enzyme assay and protein determination

Standard assays to detect enzymatic activity were performed in 100 mM triethanolamine (TEA) buffer pH 7.5 with 5 mM DTT in cuvettes with either 1 cm or 1 mm path length, depending on the concentration of substrate. Excluding studies of enzymatic activity and stability temperature dependence, all activity assays were performed with samples that were either pre-equilibrated to 25 °C, using a thermomixer (Eppendorf; Hamburg, Germany) or made and used directly at room temperature. Initial activity was measured by following the absorbance change using a Beckman Coulter DU 800 UV/Vis spectrophotometer at 340 nm. Activity of the enzyme was calculated using an extinction coefficient ε of NAD(P)H as 6.22 mM^{-1} cm^{-1} [15]. Unless otherwise noted, a substrate concentration of 0.2 mM NAD(P)H and enzyme concentration of 4 nM was used for assays. One unit (U) of activity is defined as μmol of $NAD(P)^+$ produced per minute.

The protein concentration was estimated by a Bradford assay [16]. BSA was used as standards and the absorbance was measured on a biophotometer (Eppendorf; Hamburg, Germany). SDS-PAGE analysis was performed to confirm the purity.

2.7. pH activity

Enzyme pH activity profiles were obtained at 25 °C using 100 mM buffers containing one of the following salts: sodium citrate from pH 4.0 to pH 6.5; sodium phosphate from pH 6.0 to pH 8.0; TEA from pH 7.0 to pH 8.0; Tris–Cl from pH 7.0 to pH 9.0; glycine from pH 9.0 to pH 10.0.

2.8. Temperature activity

The dependence of the enzymatic activity on temperature was studied by preheating the buffer to different temperatures, and then adding the enzyme. After 1 min of incubation, the standard assay was carried out. A temperature range of 10–55 °C was chosen for this study.

2.9. Temperature stability

Temperature stability was studied by incubating the enzyme at various temperatures for 30 min. The enzyme solution was then cooled down and assayed at 25 °C. This study covered a range of 15–55 °C.

2.10. Kinetic parameters

Depending on the enzyme, a substrate concentration range from 1.5 μM up to 984 μM was investigated to determine the k_{cat} and K_M values for NAD(P)H. This was conducted at atmospheric concentrations of oxygen, 0.25 mM, present in the system. Doubly concentrated solutions were prepared by adding each the substrate and enzyme to 100 mM TEA buffer pH 7.5. The reaction was initiated by mixing the two solutions. The specific activity was measured, and the kinetic parameters were calculated from that data.

Inhibition effects were measured by incubating the enzyme with NAD^+ for 30 min before the assay. A range of 0.2, 0.3, 0.4 and 0.6 mM were chosen and investigated.

2.11. Amplex Red Assay (H_2O_2 presence)

An Amplex Red Hydrogen Peroxide/Peroxidase Assay Kit (Invitrogen; Carlsbad, CA) was used to determine the amount of hydrogen peroxide (H_2O_2) produced during turnover. The presence of H_2O_2 was determined by incubating the standard assay mixture with Amplex Red and peroxidase. Produced resorufin is detected with an extinction coefficient ε of 54,000 M^{-1} cm^{-1} via fluorescence spectroscopy with maximal emission at 587 nm and indicates H_2O_2 production with strict 1:1 stoichiometry. Various amounts of substrates were reacted and assayed to detect the presence of H_2O_2. The reactions were carried out in the provided 50 mM sodium phosphate buffer pH 7.4. Standards for the calibration curve were prepared with the same reaction buffer. Steady-state emission and excitation spectra were recorded with a PTI fluorimeter (Birmingham, NJ).

2.12. Total turnover number (TTN)

Standard kinetic assays at pH 7.5 and 25 °C in air-saturated solution were performed with 0.25, 0.5 and 1.0 nM of enzyme. 0.2 mM NAD(P)H substrate concentration was used. Assays were carried out for 2–3 h until there was no more enzymatic conversion of the substrate. Calculations of TTN were performed by dividing the change of NAD(P)H concentration until activity reached a standstill by the (necessarily very low) concentration of enzyme subunits that was used for each assay. As the stock solution of enzyme contained DTT, the buffer was exchanged to 10 mM Tris–Cl pH 7.5.

3. Results and discussion

3.1. Cloning, expression, and purification

NoxV was identified through a sequence blast search. It has high similarity and identity levels with many other water-forming NADH oxidases (Table 1). The NoxV gene was cloned from genomic DNA of ATCC 10012 and inserted into a pET-28a vector using restriction sites NcoI and XhoI. Sequencing results of the gene showed a silent mutation where the nucleotide at position 45 changed from C to T (accession number: Q88SH4).

NoxV was overexpressed in *E. coli* BL21(DE3)pLysS constituting 8% of cell protein. Purification of NoxV resulted in a yield of 14% of the total units and a 12.7-fold increase of specific activity to 167.5 U mg^{-1} (Table 2). The pure protein was identified as a single band at 49 kDa in sodium dodecyl sulfate polyacrylamide gel electrophoresis (SDS-PAGE) analysis (lane 5, Fig. 2).

3.2. Enzyme activity and stability

NAD(P)H oxidases are used exclusively in cofactor regeneration because their byproducts, water and hydrogen peroxide, are not of interest. As utility of NADH oxidases can only be derived through coupling with other enzymes, their operating conditions must be able to match those of the cofactor consuming enzyme. Consequently, studies of reaction conditions, especially in terms of pH value and temperature, are required to maximize production and stability of both enzymes.

NoxV showed a rather broad pH activity range. Maximum activity was found at pH 7.5, independent of buffer type. The enzyme's optimal activity range was from pH 5.5 to 8.0, a common range for NAD(P)H oxidases (Fig. 3). The upper limit is compatible with most dehydrogenases, so appropriate coupling seems feasible.

The temperature activity profile showed that maximum instantaneous activity was found at 40 °C, and the activity quickly declined to zero beyond that temperature (Fig. 4). Using an Arrhenius model and data between 10 and 38 °C, the activation energy E_a was calculated as 32.7 kJ mol^{-1}, and the deactivation energy (40–55 °C) E_d was calculated as −93.6 kJ mol^{-1}. The temperature that exhibited half of the original activity after 30 min, $T_{50}{}^{30}$, was estimated to be 45 °C (Fig. 5). At 55 °C the enzyme was completely inactive. The enthalpy of deactivation, ΔH_d, was calculated using the Van't Hoff equation to be 5.0 kJ mol^{-1} (Fig. 5).

Table 1
Sequence identity and similarity comparison of water forming NADH oxidases from different bacteria with respect to NoxV from *L. plantarum* (accession number: Q88SH4).

Bacteria	Identity (%)	Similarity (%)	Accession number	Reference
Lactobacillus sanfranciscensis	59.4	72.2	Q9F1X5	[18]
Lactococcus lactis	33.1	56.1	A2RIB7	[9]
Lactobacillus brevis	64.0	74.2	Q8KRG4	[12]
Enterococcus faecalis	33.0	42.9	P37061	[27]
Streptococcus mutans	9.4	19.8	Q54453	[28]

Table 2
Table of purification.

	Volume (ml)	Units (U)	Protein (mg)	Sp. ac. (U mg^{-1})	Purification fold	Yield (%)
Lysate	20	1843.5	139.3	13.24	1.0	100
AS50 dia.	7	930.0	88.5	10.51	0.8	50
Butyl dia.	37.5	379.3	4.7	80.72	6.1	21
DEAE	20	261.9	1.6	167.5	12.7	14

Lysate: clarified lysate; AS50 dia.: supernatant from centrifuged sample dialyzed against 50% ammonium sulfate; butyl dia.: fractions collected from HiPrep 16/10 butyl column dialyzed against 10 mM Tris-Cl and 5 mM DTT; DEAE: fractions collected from HiPrep 16/10 DEAE column.

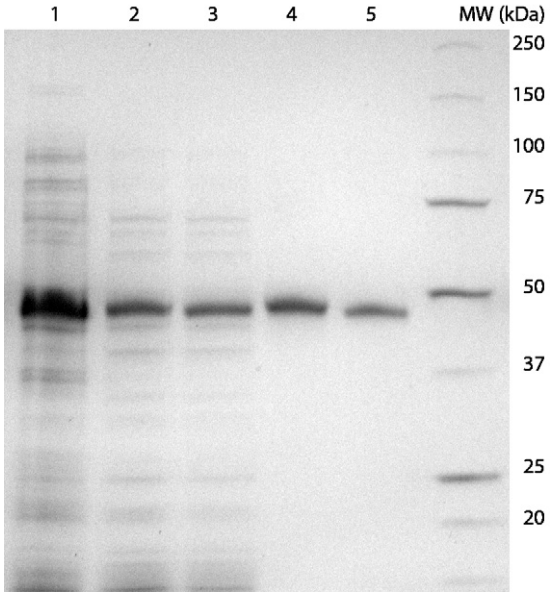

Fig. 2. SDS-PAGE analysis of NoxV. Lane 1: 15 μg lysate, lane 2 and 3: 6 and 3 μg, respectively, of dialyzed protein collected from HiPrep 16/10 butyl column, lane 4 and 5: 3 and 1 μg, respectively, of collected protein from HiPrep 16/10 DEAE column. The desired protein band is approximately 49 kDa.

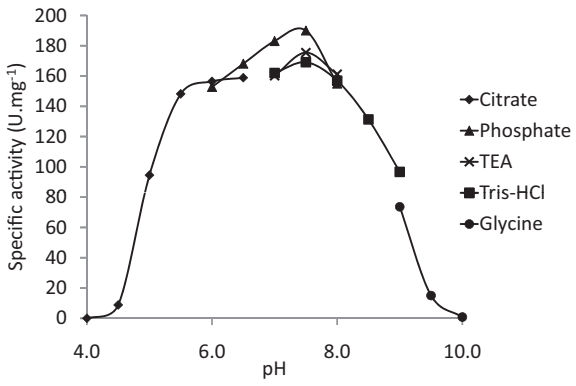

Fig. 3. *L. plantarum* NoxV activity profile in different buffers (100 mM) at different pH values at 25 °C.

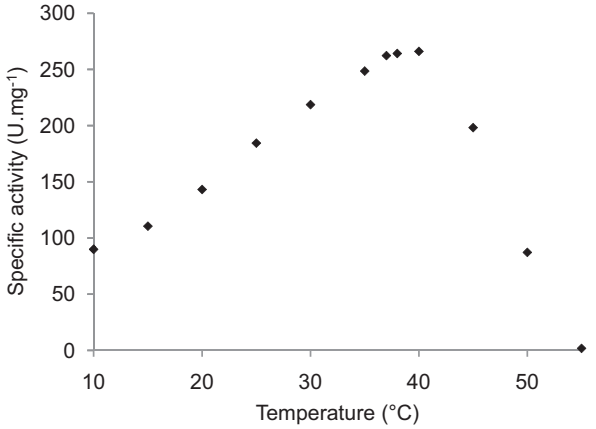

Fig. 4. *L. plantarum* NoxV activity profile at various temperatures with 100 mM TEA buffer pH 7.5.

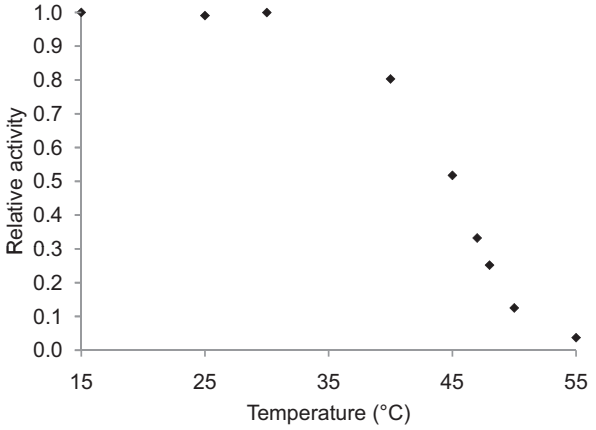

Fig. 5. $T_{50}{}^{30}$ plot. Checking stability of *L. plantarum* NoxV by incubating at different temperatures for 30 min each.

3.3. Kinetic parameters

Apparent kinetic data were obtained at constant oxygen concentration (air saturation) at 25 °C and pH 7.5 over a concentration range of NADH from 5 to 200 μM. The data were fitted with four different models (non-linear Michaelis–Menten, Lineweaver–Burk, Eadie–Hofstee, and Hanes–Woolf), all of which were in good agreement. Through non-linear fitting with a least squares approx-

Table 3
Comparison of TTN with and without DTT, for NADH oxidases from *L. plantarum*, *L. sanfranciscensis* and *L. lactis*.

Organism	Enzyme	NADH		NADPH	
		TTN	TTN with DTT	TTN	TTN with DTT
L. plantarum	NoxV WT	128,000	168,000	–	–
	L179R	181,000	148,000		
	G178R/L179R	123,000	162,000	100,000	107,000
L. sanfranciscensis [4]	Nox2	5000	112,500		
L. lactis [9]	Nox2	38,740	78,480	–	–

For all the TTN measurements the relative standard deviation (%RSD) was less than 5%, except for the TTN of mutant G178R/L179R with NADH, which was 12%.

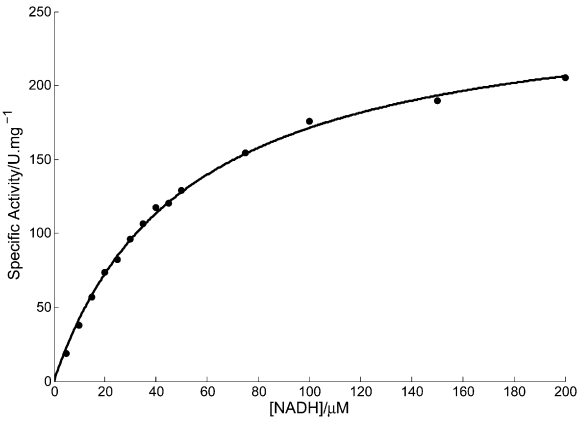

Fig. 6. Nonlinear fitting to a Michaelis–Menten kinetic to determine the kinetic parameters k_{cat} and K_M at pH 7.5, 25 °C.

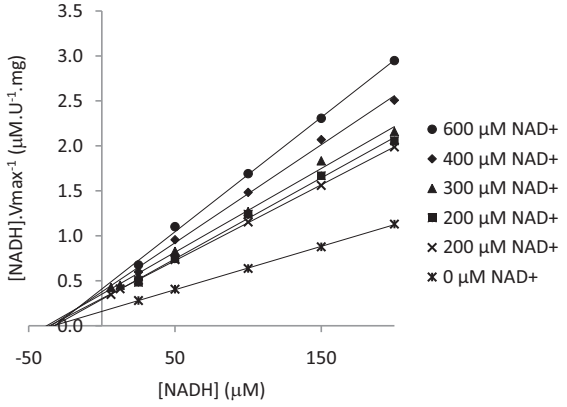

Fig. 7. Hanes–Woolf plot to identify NAD^+ inhibition.

imation, the apparent k_{cat} and K_M values of the wild type were measured to be 211.6 s^{-1} and 50.2 μM, respectively, with an R^2 of 0.998 (Fig. 6).

Possible product inhibition was investigated by incubating the enzyme with different concentrations of NAD^+. A non-competitive inhibition pattern was observed where the v_{max} value decreased with increasing inhibitor concentration, while $K_{M,app}$ was constant. The product inhibition constant, K_{IP}, was calculated to be 289 μM for NAD^+ (Fig. 7). The apparent inhibition ratio $K_{M,app}/K_{IP}$ is calculated to be 0.17. As this ratio is less than unity, it indicates that complete conversion is possible despite the non-competitive product inhibition [17].

3.4. Water/H_2O_2 formation

The Amplex Red assay was performed to determine whether NoxV is a water- or hydrogen peroxide-producing enzyme. H_2O_2 was formed in 2.63% of the catalytic events, slightly higher than the analogs from *Lactobacillus sanfranciscensis* (0.2%) and *Lactococcus lactis* (0.4–0.7%) [9,18], thus strongly suggesting that NoxV is a water-forming oxidase.

Table 4
Cell lysate activity of mutants.

Mutant	NADH activity (U/mg)	NADPH activity (U/mg)
Wild type	10.0	0.00
G178K	3.92	0.46
G178R	1.51	0.23
L179K	5.14	1.03
L179R	7.32	1.76
L179H	1.37	0.64
G178K/L179K	0.84	3.11
G178K/L179R	2.00	5.68
G178K/L179H	1.24	3.85
G178R/L179K	0.94	3.56
G178R/L179R	2.64	6.00
G178R/L179H	0.64	0.52

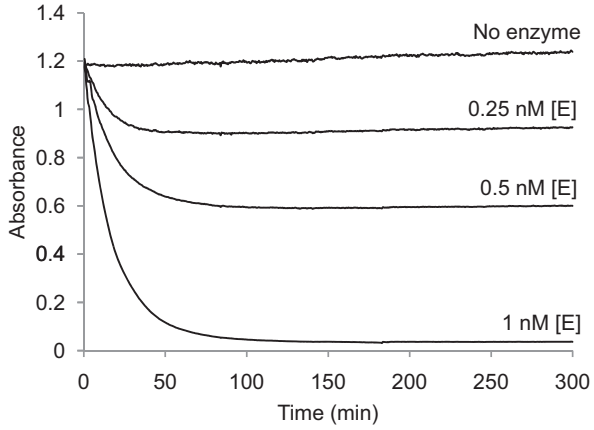

Fig. 8. Total turnover number analysis with different amounts of enzyme. The reaction was carried on until there was no consumption of substrate ([E] = 0.25, 0.5 and 1.0 nM, 25 °C, pH 7.4).

3.5. Total turnover number (TTN)

Total turnover number (TTN) is a measure of catalyst productivity, defined as the total amount of product produced over the lifetime of an enzyme [19]. The TTN, in presence of DTT, was found to be approximately 168,000, at 25 °C and pH 7.5 (Fig. 8).

Three potential causes of TTN limitation, which are commonly associated with enzyme deactivation, were investigated: (i) thermal deactivation at 25 °C, (ii) deactivation caused by H_2O_2, and (iii) non-competitive product (NAD^+) inhibition in the system. Thermal stability at 25 °C (i) was measured by incubating the enzyme for extended periods of time. The enzyme was then assayed to determine the remaining activity. As there was no enzymatic activity loss after 2 h (data not shown), which is longer than the reaction completion timescale (Fig. 8), this study proved that the enzyme

Table 5
Kinetic parameters of wild-type(WT) and mutant NAD(P)H oxidases. Data were fitted with least squares approximation to Michaelis–Menten kinetics with an R^2 of 0.96 or higher.

Enzyme	NADH			NADPH		
	k_{cat} (s^{-1})	K_M (μM)	k_{cat}/K_M ($\mu M^{-1}\ s^{-1}$)	k_{cat} (s^{-1})	K_M (μM)	k_{cat}/K_M ($\mu M^{-1}\ s^{-1}$)
WT	211.6	50.2	4.22	–	–	–
L179R	122.0	6.56	18.6	146.4	489.6	0.30
G178R/L179R	34.0	2.57	13.2	114.1	9.76	11.7

became catalytically inactive before it began to thermally deactivate. The effect of H_2O_2 was studied (ii) at 25 °C and pH 7.5 within a concentration range from 25 to 200 μM. Even at high concentrations of H_2O_2 the specific activity did not change over 1 h (data not shown), thus demonstrating that the enzyme is indeed stable against H_2O_2. The presence of NAD^+ inhibition (iii) and its pattern had been elucidated (see Section 2.10). However, as expected from the apparent inhibition ratio of 0.17, even at high concentrations of NAD^+ there was a reasonable amount of residual activity (data not shown), so it cannot be concluded that NAD^+ had inhibited the reaction completely. The cause of TTN-coupled deactivation is still not fully elucidated but it is not related to temperature nor either H_2O_2 or NAD^+ concentration.

To investigate the effect of reducing agents on the TTN, measurements were taken with and without reducing agents. The TTN without reducing agents, with 5 mM DTT, and with 5 mM BME were 128,000, 168,000, and 107,000, respectively. The presence of DTT had a positive effect but it was not as dramatic compared to the NADH oxidase from *L. sanfranciscensis*, which has an increase of over 20-fold [4]. However, addition of BME decreased the TTN by ~15%. The reason for the different influence of the reducing agents on the TTN is unknown, and will be assessed in future studies. One intriguing but speculative thought focuses on the different stoichiometry of the sulfenic acid reduction for DTT and BME: a single molecule of DTT is capable of performing reduction, whereas two molecules of BME are required. In contrast, the first molecule of BME initiates thiol-disulfide interchange and occupies the water channel, thus blocking access to the second BME molecule and leaving the residue inactive.

NoxV has shown a higher TTN compared to previously studied NADH oxidases from *L. sanfranciscensis* and *L. lactis*, both with and without exogenously added reducing agents (Table 3). Such a higher TTN is an indication of improved intrinsic stability against overoxidation at the catalytically active cysteine residue because DTT, a known enhancer of TTN in the other NADH oxidases from *L. sanfranciscensis* and *L. lactis*, has little effect on the TTN in *L. plantarum*. As overoxidation of a catalytic cysteine is known as limiting catalysis over time in enzymes such as D-amino acid oxidase from *Trigonopsis variabilis* and xenobiotic reductase A (xen A) from *Pseudomonas putida*, this increased intrinsic stability is of great interest [20,21]. Since there are known inhibition effects of DTT on certain rare sugar-producing dehydrogenases, such as mannitol dehydrogenase from *Apium graveolens*, it is crucial for a generally useful NAD(P)H oxidase to be stable without DTT [22]. Also, improved stability without reducing agents would be a significant advantage in industries where the use of reducing agents is avoided.

3.6. Mutation for NADPH activity

Wild type NoxV had activity exclusively towards NADH and not towards NADPH. To introduce NADPH activity, substrate binding pocket mutations were carried out. Homology modeling of the sequence of NoxV from *L. plantarum* onto the crystal structure of NAD(P)H oxidase from *L. sanfranciscensis* [23] revealed electrostatic differences in the substrate binding pocket. Nox2 from *L. sanfranciscensis* features histidine (His 179) able to accommodate the negative charge of the 2′-phosphate, but NoxV consists of only small or hydrophobic residues in that area. Based on this knowledge, these residues were targeted for mutation with basic residues such as histidine, lysine and arginine [24,25,29].

The single mutations of residues G178 and L179 into K, R and K, R, H, respectively, and double mutations 178/179 were performed and investigated for substrate specificity. The mutation of G178H was excluded because then two histidines would be positioned next to each other, causing steric hindrance within the binding pocket. The resulting mutants were expressed on small scale and assayed at the cell lysate level (Table 4). All the mutants showed activity with both NADH and NADPH as substrates. Among the single and double variants, L179R shows the highest specific activity at 25 °C and pH 7.5 with NADH (7.32 U/mg) and G178R/L179R with NADPH (6.00 U/mg), compared to wild-type at 10.0 U/mg. We surmise that introduction of an additional positive charge at G178R stabilizes the positioning of L179R, decreasing the ability of free rotation of L179R side-chain bonds through hydrogen bonding. Arginine may be expected to provide the greatest NADPH activity because it has the most positions for hydrogen bonding. The low activity of L179H can be rationalized by the presence of an adjacent proline causing steric hindrance.

3.7. Study of variants L179R and G178R/L179R

L179R and G178R/L179R were selected for further purification and kinetic characterization (Table 5). L179R was not as active as the wild-type (lower $k_{cat,NADH}$). However, the $K_{M,NADH}$ value was also much lower, improving the specificity $k_{cat,app}/K_{M,NADH}$ more than 4-fold. The mutant also showed NADPH activity but with a very high $K_{M,NADPH}$ value. The double mutant G178R/L179R shows a trend similar to L179R: decreased $k_{cat,app,NADH}$ and $K_{M,NADH}$ values, resulting in an improved specificity $k_{cat,app}/K_{M,NADH}$ of 13.2 $\mu M^{-1}\ s^{-1}$. For NADPH activity $k_{cat,app}/K_{M,NADPH}$ was 11.7 $\mu M^{-1}\ s^{-1}$. Overall, both variants yielded improved specificities $k_{cat,app}/K_M$ for both NADH and NADPH. The TTN of the two variants behaved similarly to the wildtype, in that the presence of reducing agents did not affect the processing stability (TTN) to a great extent (Table 3).

4. Conclusion

Starting from an annotated sequence, NADH oxidase V from *L. plantarum* (ATCC 10012) was developed and demonstrated to be a very active enzyme in air-saturated aqueous buffer at pH 7.5 and 25 °C ($k_{cat,app}$ = 212 s^{-1} and $K_{M,app}$ = 50.2 μM). The temperature and pH optima, 45 °C and pH 5.5–8.0, respectively, overlap with relevant dehydrogenases that might be coupled for cofactor regeneration with NoxV. With total turnover numbers (TTN) of 128,000 and 168,000, respectively, in the absence and presence of DTT, *L. plantarum* NoxV demonstrated high processing stability regardless of the presence of reducing agents, a first among NADH oxidases.

After inspection of the homology model of *L. plantarum* NoxV on the structure of the *L. sanfranciscensis* analog, mutations in the substrate binding pocket to basic amino acid residues to accommodate the negative charge of the 2′-phosphate of NADPH were intro-

duced to broaden the substrate specificity to NADPH. All single and double variants G178K,R/L179K,R,H exhibited significant NADPH and NADH activity. Novel and more stable cofactor regeneration enzymes, in conjunction with novel methods of immobilization, such as on functionalized nanotubes [26], stand to further broaden the application of oxidative reactions with dehydrogenases/NADH oxidases.

References

[1] R.D. Woodyer, N.J. Wymer, F.M. Racine, S.N. Khan, B.C. Saha, Appl. Environ. Microb. 74 (2008) 2967–2975.
[2] E. Riedel, M. Nundel, H. Hampl, Nephron 74 (1996) 261–265.
[3] V. Teplan, O. Schuck, M. Votruba, R. Poledne, L. Kazdova, J. Skibova, J. Maly, Wien Klin Wochenschr 113 (2001) 661–669.
[4] P. Odman, W.B. Wellborn, A.S. Bommarius, Tetrahedron – Asymmetry 15 (2004) 2933–2937.
[5] M.D. Leonida, Curr. Med. Chem. 8 (2001) 345–369.
[6] H.K. Chenault, G.M. Whitesides, Appl. Biochem. Biotechnol. 14 (1987) 147–197.
[7] W.A. van der Donk, H.M. Zhao, Curr. Opin. Biotechnol. 14 (2003) 421–426.
[8] M. Higuchi, Y. Yamamoto, L.B. Poole, M. Shimada, Y. Sato, N. Takahashi, Y. Kamio, J. Bacteriol. 181 (1999) 5940–5947.
[9] R.R. Jiang, B.R. Riebel, A.S. Bommarius, Adv. Synth. Catal. 347 (2005) 1139–1146.
[10] B. Geueke, B. Riebel, W. Hummel, Enzyme Microb. Technol. 32 (2003) 205–211.
[11] C.M. Gibson, T.C. Mallett, A. Claiborne, M.G. Caparon, J. Bacteriol. 182 (2000) 448–455.
[12] W. Hummel, B. Riebel, Biotechnol. Lett. 25 (2003) 51–54.
[13] L.B. Poole, A. Claiborne, J. Biol. Chem. 264 (1989) 12330–12338.
[14] A. Claiborne, J.I. Yeh, T.C. Mallett, J. Luba, E.J. Crane, V. Charrier, D. Parsonage, Biochemistry-Us 38 (1999) 15407–15416.
[15] R.M.C. Dawson, Data for Biochemical Research, 3rd ed., Clarendon Press, Oxford, 1986.
[16] M.M. Bradford, Anal. Biochem. 72 (1976) 248–254.
[17] L.G. Lee, G.M. Whitesides, J. Org. Chem. 51 (1986) 25–36.
[18] B.R. Riebel, P.R. Gibbs, W.B. Wellborn, A.S. Bommarius, Adv. Synth. Catal. 344 (2002) 1156–1168.
[19] A.S. Bommarius, B.R. Riebel, Biocatalysis, Wiley-VCH, Weinheim/Cambridge, 2004.
[20] A. Slavica, I. Dib, B. Nidetzky, Appl. Environ. Microb. 71 (2005) 8061–8068.
[21] Y. Yanto, H.H. Yu, M. Hall, A.S. Bommarius, Chem. Commun. 46 (2010) 8809–8811.
[22] J.M.H. Stoop, J.D. Williamson, M.A. Conkling, J.J. MacKay, D.M. Pharr, Plant Sci. 131 (1998) 43–51.
[23] G.T. Lountos, R.R. Jiang, W.B. Wellborn, T.L. Thaler, A.S. Bommarius, A.M. Orville, Biochemistry-Us 45 (2006) 9648–9659.
[24] P. Bubner, M. Klimacek, B. Nidetzky, FEBS Lett. 582 (2008) 233–237.
[25] R. Woodyer, W.A. van der Donk, H.M. Zhao, Biochemistry-Us 42 (2003) 11604–11614.
[26] L.A. Wang, L. Wei, Y.A. Chen, R.R. Jiang, J. Biotechnol. 150 (2010) 57–63.
[27] R.P. Ross, A. Claiborne, J. Mol. Biol. 227 (1992) 658–671.
[28] J. Matsumoto, M. Higuchi, M. Shimada, Y. Yamamoto, Y. Kamio, Biosci. Biotechnol. Biochem. 60 (1996) 39–43.
[29] O. May, Presentation at Biocat 2010, Hamburg, Germany.